Research in Astronomy and Astrophysics, 25:025019 (9pp), 2025 February

https://doi.org/10.1088/1674-4527/adae45
CSTR: 32081.14.RAA.adae45

Model—Independent Probe of Cosmic Distance Duality Relation

Savita Gahlaut
Deen Dayal Upadhyaya College, University of Delhi, Sector-3, Dwarka, New Delhi 110078, India; savitagahlaut@ddu.du.ac.in
Received 2024 September 7; revised 2024 December 20; accepted 2025 January 21; published 2025 February 20

Abstract

In this paper, cosmic distance duality relation (CDDR) is probed without considering any background cosmological model. The only a priori assumption is that the Universe is described by the Friedmann–Lemaître–Robertson–Walker (FLRW) metric. The strong gravitational lensing data is used to construct the dimensionless comoving distance function $d(z)$ and latest type Ia supernovae Pantheon+ data is used to estimate luminosity distances at the corresponding redshifts z. Using the distance sum rule along null geodesics of the FLRW metric, the CDDR violation is probed in both flat and non-flat spacetime by considering two parametrizations for $\eta(z)$, the function generally used to probe the possible deviations from CDDR. The results show that CDDR is compatible with the observations at a very high level of confidence for linear parametrization in a flat Universe. In a non-flat Universe too, CDDR is valid within the 1σ confidence interval with a mild dependence of η on the curvature density parameter Ω_K. The results for nonlinear parametrization also show no significant deviation from CDDR.

Key words: cosmology: observations – gravitational lensing: strong – (cosmology:) distance scale

1. Introduction

The cosmic distance duality relation (CDDR) is one of the fundamental relations in cosmology based on the Etherington reciprocity relation (Etherington 1933). If one assumes the spacetime geometry to be Riemannian and the number of photons to be conserved along the null geodesics, the CDDR relates the luminosity distance (D_L) and angular diameter distance (D_A) at the same redshift z as

$$\eta(z) \equiv \frac{D_L(z)}{D_A(z)}(1+z)^{-2} = 1. \quad (1)$$

The CDDR is valid irrespective of which cosmological model is used to describe the Universe. Many cosmological observations, such as Cosmic Microwave Background Radiation, galaxy clusters and gravitational lensing, are based on this fundamental relation. Further, it has been used, assuming it to be true, to study galaxy cluster physics, i.e., the possible morphologies of galaxy clusters (Holanda et al. 2011, 2012), the temperature profile, the gas mass density profile of galaxy clusters (Cao & Zhu 2011; Cao et al. 2016) and so on. However CDDR may be violated due to photon absorption by dust (Corasaniti 2006), coupling of photons with non-standard particles (Bassett & Kunz 2004), gravitational lensing, variations in fundamental constants (Ellis et al. 2013) or simply due to systematic observational errors (Holanda et al. 2013). Any violation of it, i.e., $\eta(z) \neq 1$, may indicate the presence of new physics in the theory of gravity or the existence of some unaccounted systematic errors in the observations. Thus it is crucial to investigate the validity of CDDR with the latest cosmological observations.

The validity of CDDR is investigated in several papers using different cosmological data sets available (Li et al. 2011; Li et al. 2013; Liao et al. 2016; Ellis et al. 2013; Holanda & Busti 2014; Rana et al. 2017; Ruan et al. 2018; Lyu et al. 2020). Some authors consider a background cosmological model while others take a model-independent approach to test CDDR. A pre-assumption of background cosmological model necessitates the optimization of 'nuisance' parameters in the distance-redshift relation. This requirement can introduce additional uncertainty and bias which can lead to conflicting results and/or wider confidence intervals (Melia 2018). Generally, luminosity distance is estimated from type Ia supernovae (SNe Ia) observations while the angular diameter distance is inferred from baryon acoustic oscillation (BAO) data, Hubble parameter data ($H(z)$), strong gravitational lensing (SGL) data, gamma-ray bursts and other astrophysical probes. The point to be noted here is that, to study the validity of CDDR, the angular diameter distance and luminosity distance need to be measured at the same redshift. To check the consistency of different independent data sets in a non-parametric way, numerical techniques, like genetic algorithms, non-parametric smoothing (NPS) technique, LOESS & SIMEX, Gaussian Processes, etc., have been used in literature to study the validity of CDDR (Ruan et al. 2018; Nesseris & Bellido 2012; Shafieloo et al. 2013; Rana et al. 2016). No significant violation of CDDR compared with the uncertainties of the observations has been reported in these studies. Still continuing to test the CDDR with latest cosmological observations is important along with looking for systematic errors among the previous analysis.

SNe Ia are considered to be the standard candles in the Universe, as they are as bright as a galaxy at their peak, and are often used as distance indicators. Recently, Scolnic et al. (2022) published the largest compilation of spectroscopically confirmed SNe Ia, named the Pantheon+ sample. The sample is from the analysis of 1701 light curves compiled across 18 different surveys of 1550 distinct SNe Ia. This sample improves upon the previous samples by not only increasing the sample size and redshift span but also by improving the treatments of systematic uncertainties. Further, with new powerful space and ground-based telescopes for imaging and spectroscopic observations, many new SGL systems have been discovered. SGL systems can be a valuable tool to constrain cosmological parameters if one has a good knowledge of the lens mass model. From various surveys (SLACS, S4TM, BELLS and BELLS GALLERY), Chen et al. (2019) compiled 161 galaxy-scale strong lensing systems, all early-type galaxies with E or S0 morphologies. In the sample only those lens galaxies were selected which do not have any significant substructure or close massive companion. These two conditions ensured that the lens galaxies are spherically symmetric.

Taking advantage of the significant improvements in SGL and SNe Ia observations, I present a new cosmological model-independent approach to probe the CDDR by jointly considering the SGL data and latest Pantheon+ SNe Ia data set. The large data size makes the data sets suitable for the statistical analysis and the constraints on CDDR are improved. In most works so far, CDDR is tested assuming a flat spacetime, whereas in this work the CDDR probe is extended to the non-flat spacetime too. Using the SGL data, the dimensionless co-moving distance function $d(z)$ is constructed to avoid the bias brought in by redshift incoincidence between the observational data sets in analysis. The continuous function $d(z)$ provides the estimate of luminosity distance $D_L(z)$. Comparing the luminosity distances derived from SNe Ia data with those estimated from SGL data, one can investigate the validity of CDDR. I take the parametric approach to probe the validity of CDDR. Using the distance sum rule, I investigate CDDR in both flat and non-flat spacetime.

The outline of the paper is as follows. The methodology to construct model-independent dimensionless co-moving distance function $d(z)$ using SGL data and combining it with SNe Ia data to estimate $\eta(z)$ is discussed in Section 2. In Section 3, SGL data and Pantheon+ data used in this work are presented. Results and conclusions are presented in Section 4 and discussion in Section 5.

2. Theory

In a homogeneous and isotropic Universe, the geometry of the spacetime can be described by the Friedmann–Lemaître–Robertson–Walker (FLRW) metric

$$ds^2 = c^2dt^2 - a(t)^2\left[\frac{dr^2}{1 - Kr^2} + r^2(d\theta^2 + \sin^2\theta\, d\phi^2)\right], \tag{2}$$

where c is the speed of light, $a(t)$ is the cosmic scale factor and K is the spatial curvature constant and is ±1 or 0 for a suitable choice of units for r.

The dimensionless transverse co-moving distance $d(z)$ in FLRW cosmology is

$$d(z) = \begin{cases} D_c, & K = 0 \\ \frac{1}{\sqrt{|\Omega_K|}}\sinh(\sqrt{|\Omega_K|}D_c), & K = -1 \\ \frac{1}{\sqrt{|\Omega_K|}}\sin(\sqrt{|\Omega_K|}D_c), & K = 1 \end{cases} \tag{3}$$

where $\Omega_K = -Kc^2/a_0^2H_0^2$, $D_c = \int_0^z \frac{H_0}{H(z')}dz'$, $H(z)$ is Hubble parameter and H_0 and a_0 are the present values of Hubble parameter and scale factor respectively. The angular diameter distance is

$$D_A(z) = \frac{c}{H_0(1 + z)}d(z), \tag{4}$$

and the luminosity distance is

$$D_L(z) = (1 + z)\frac{c}{H_0}d(z). \tag{5}$$

2.1. Strong Gravitational Lensing

Multiple images of a background galaxy (source) appear due to the lensing effect of a galaxy or cluster of galaxies (lens) along the line of sight. A ring-like structure, called Einstein ring, is formed if the source, lens and observer are perfectly aligned along the same line of sight. The multiple image separation or the radius of Einstein ring, in case of perfect alignment, in a specific strong lensing system depends only on angular diameter distances from observer to the lens, lens to source and to the source, provided a reliable model for the mass distribution within the lens is known. A Singular Isothermal Ellipsoid (SIE) model, in which the projected mass distribution is elliptical (Ratnatunga et al. 1999), is often used for the purpose. As most of the lensing galaxies observed are elliptical (early-type), the SIE model is quite reasonable (Kochanek et al. 2000). A simpler Singular Isothermal Sphere (SIS) model, an SIE with zero ellipticity, is also found to be consistent with the observations (Cao et al. 2015; Melia et al. 2015). The Einstein ring radius $\theta_{\rm E}$ in an SIS lens is (Schneider et al. 2006)

$$\theta_{\rm E} = 4\pi\frac{\sigma_{\rm SIS}^2}{c^2}\frac{D_{ls}}{D_s}, \tag{6}$$

where c is the speed of light, $\sigma_{\rm SIS}$ is the stellar velocity dispersion in the lensing galaxy and D_{ls}/D_s is the ratio of the angular diameter distance between source and lens and between source and observer. If one has the values of $\theta_{\rm E}$ from image astrometery and $\sigma_{\rm SIS}$ from spectroscopy, the distance ratio $D^{\rm ob}(z_l, z_s) = \frac{D_{ls}}{D_s}$ can be estimated.

2.2. Distance Sum Rule

The ratio of angular diameter distances D_{ls} and D_s in Equation (6) can be expressed in terms of the corresponding dimensionless co-moving distances $d(z)$ as

$$D(z_l, z_s) = \frac{d_{ls}}{d_s}. \tag{7}$$

If $d(z)$ is monotonic and $d'(z) > 0$, then d_{ls} and d_s are related by the distance sum rule (Peebles 1993; Räsänen et al. 2015)

$$d_{ls} = d_s\sqrt{1 + \Omega_K d_l^2} - d_l\sqrt{1 + \Omega_K d_s^2}. \tag{8}$$

Therefore,

$$D(z_l, z_s) = \sqrt{1 + \Omega_K d_l^2} - \frac{d_l}{d_s}\sqrt{1 + \Omega_K d_s^2}. \tag{9}$$

Using the distance ratio values $D(z_l, z_s)$, obtained from SGL observations, a continuous distance function $d(z)$ can be constructed in a cosmological model-independent way using a polynomial fit (Räsänen et al. 2015; Collet et al. 2019; Wei & Melia 2020; Qi et al. 2021). Here, a third order polynomial

$$d(z) = z + a_1 z^2 + a_2 z^3, \tag{10}$$

with the initial conditions $d(0) = 0$ and $d'(0) = 1$, is constructed by fitting the SGL data.

2.3. SNe Ia as Standard Candles

SNe Ia, due to their superior brightness, are often adopted to provide the most effective method to measure luminosity distances. The distance modulus μ of a supernova is defined as

$$\mu^{\rm th}(z) = m - M' = 5\log(D_L/{\rm Mpc}) + 25, \tag{11}$$

where m is the apparent magnitude, M' is the absolute magnitude and D_L is the luminosity distance. Using the distance duality equation,

$$\mu^{\rm th}(z) = m - M' = 5\log\left(\frac{\rm c}{\rm H_0}(1 + {\rm z})\,\eta({\rm z})\,{\rm d(z)}\,/\,{\rm Mpc}\right) + 25. \tag{12}$$

To test the violation of CDDR, I use the following parametrizations of $\eta(z)$:

$$\text{(i)} \quad \eta(z) = 1 + \eta_0 z,$$

and

$$\text{(ii)} \quad \eta(z) = 1 + \frac{\eta_0 z}{1 + z}.$$

3. Data and Methodology

SGL data used in this study is taken from the catalog of 161 galaxy-scale source SGL systems, compiled by Chen et al. (2019), from the LSD, SL2S, SLACS, S4TM, BELLS and BELLS GALLERY surveys. Only early-type lens galaxies with E or S0 morphologies which do not have any significant substructure or a close massive companion are selected for the sample. These two conditions ensure that the lens galaxies in the sample are spherically symmetric. For each lens, the source redshift (z_s), lens redshift (z_l) and luminosity averaged central velocity dispersion measured within the aperture $\sigma_{\rm ap}$ are determined spectroscopically. As the lenses in the sample are from different surveys, $\sigma_{\rm ap}$ is normalized to the velocity dispersions within circular aperture of radius $R_{\rm eff}/2$, where $R_{\rm eff}$ is the half-light radius of the lens. The normalized velocity dispersion σ_0 is (Jorgensen et al. 1995a,1995b; Cappellari et al. 2006)

$$\sigma_0 = \sigma_{\rm ap}\,(\theta_{\rm eff}/(2\theta_{\rm ap}))^{\nu}, \tag{13}$$

where $\theta_{\rm eff} = R_{\rm eff}/D_l$ and ν is the correction factor to be fitted from the samples of observations. Following Jorgensen et al. (1995a, 1995b), I take $\nu = -0.04$. Since it has been established that the intermediate-mass early-type elliptical lens galaxies show the best consistency with the SIS lens model (Cao et al. 2016; Koopmans et al. 2006, 2009; Treu et al. 2006), I select only those systems from the catalog whose velocity dispersion is in the range $200\,{\rm km\,s^{-1}} \leqslant \sigma_{\rm ap} \leqslant 300\,{\rm km\,s^{-1}}$. As the velocity dispersion for an SIS model $\sigma_{\rm SIS}$ may not be same as the central velocity dispersion σ_0, a new parameter $f_{\rm E}$ was introduced by Kochanek (Kochanek 1992) such that $\sigma_{\rm SIS} = f_{\rm E}\sigma_0$. The parameter $f_{\rm E}$ compensates for the contribution of dark matter halos in velocity dispersion, systematic errors in measurement of image separation and any possible effect of background matter over lensing systems. All these factors can affect the image separation by up to 20% which limits $\sqrt{0.8} < f_{\rm E} < \sqrt{1.2}$ (Cao et al. 2012; Ofek et al. 2003). In the present analysis, $f_{\rm E}$ is taken as a free-parameter and is fitted along with the other parameters (Gahlaut 2024).

The Einstein radius $\theta_{\rm E}$ is determined by fitting model mass distributions to generate model lensed images and comparing them to the observed images taken from Hubble Space Telescope or from Earth-based telescopes. The relative uncertainty in $\theta_{\rm E}$ is taken to be 5% for all lenses (Cao et al. 2016). Finally, from the catalog of SGL systems I also exclude the systems for which the distance ratio $D^{\rm ob} > 1$, as they are not physical (see Equation (8)). The distribution of data points in the catalog with $\sigma_{\rm ap}$ and $D^{\rm ob}$ is shown in Figure 1.

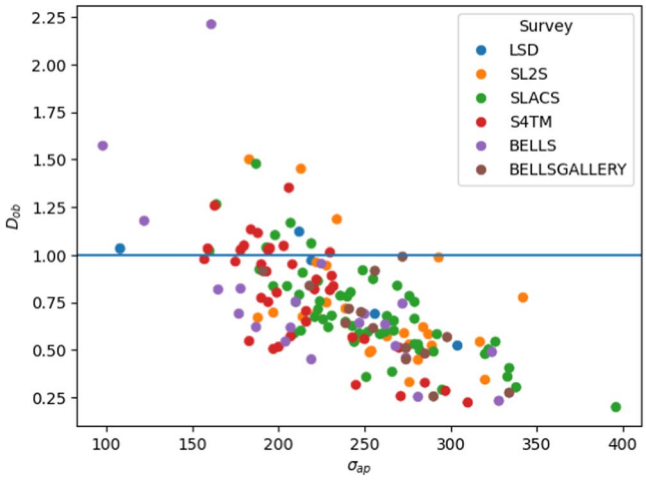

Figure 1. From the catalog of 161 SGL systems, only those systems which show best consistency with the SIS lens model (for which $200\,\mathrm{km\,s^{-1}} \leqslant \sigma_{\rm ap} \leqslant 300\,\mathrm{km\,s^{-1}}$) are chosen. Further, the lens systems with the observed distance ratio $D_{\rm ob} > 1$ (being unphysical) are excluded.

The likelihood function for the SGL data set is

$$L = e^{-\chi_1^2/2}, \tag{14}$$

where

$$\chi_1^2 = \sum_{i=1}^{N} \left(\frac{D^{\rm th}(z_{l,i}, z_{s,i}, a_1, a_2) - D^{\rm ob}(\sigma_{0,i}, \theta_{{\rm E},i})}{D^{\rm ob}\Delta D^{{\rm ob})_i}} \right)^2, \tag{15}$$

here $N = 102$ is the number of data points for which $D^{\rm ob} < 1$ and velocity dispersion is in the range $200\,\mathrm{km\,s^{-1}} \leqslant \sigma_{\rm ap} \leqslant 300\,\mathrm{km\,s^{-1}}$. $\Delta D^{\rm ob}$ is the uncertainty in the value of $D^{\rm ob}$ given by

$$\Delta D^{\rm ob} = \sqrt{\left(\frac{\Delta\theta_{\rm E}}{\theta_{\rm E}}\right)^2 + 4\left(\frac{\Delta\sigma_0}{\sigma_0}\right)^2}, \tag{16}$$

where $\Delta\theta_{\rm E}$ and $\Delta\sigma_0$ are the uncertainties in the measurement of Einstein radius and velocity dispersion respectively.

The Pantheon+ sample, recently published by Scolnic et al. (2022), is used to estimate the luminosity distance $D_L^{\rm ob}(z)$. Scolnic et al. reported the corrected apparent magnitude $m^{\rm corr} = \mu^{\rm ob} + M_B$ by analyzing 1701 supernova light curves from 1550 distinct SNe Ia ranging in redshift from $z = 0.001$ to 2.26 and fitting them using a SALT2 model. To reduce the systematic uncertainties of the data set, the BEAMS method with bias corrections is used (Kessler & Scolnic 2017) to make corrections to selection biases and contamination from core-collapse SNe. The uncertainties, including statistical and systematic uncertainties, for the data are given by the 1701×1701 covariance matrix C (Brout et al. 2022; Riess et al. 2022). The covariance matrix C accounts for the errors from the measurement of redshifts, peculiar velocities of host galaxies, calibration of light curves and the SALT2 model fitting, extinction due to the Milky Way, and simulations of survey modeling, distance modulus uncertainty modeling, and intrinsic scatter models.

The chi-square function for the supernovae Pantheon+ sample is

$$\chi_2^2 = \triangle\mu^{\dagger} \cdot \boldsymbol{C^{-1}} \cdot \triangle\,\mu, \tag{17}$$

where $\triangle\mu_i = \mu^{\rm th}(z_i, \boldsymbol{p}) - \mu^{ob}(z_i)$ is the vector of residuals of the sample and $\boldsymbol{p} = (\Omega_K, \eta_0, a_1, a_2, M)$ is the vector formed by the parameters to be fitted from the data. Given the degeneracy of factor $5\log_{10}(c/H_0{\rm Mpc}) + 25$ with absolute magnitude M', both are combined and fitted as the parameter $M = M' + 5\log_{10}(c/H_0{\rm Mpc}) + 25$.

The combined log-likelihood function for the SGL and SNe data sets is

$$\ln(L_{\rm tot}) = -0.5(\chi_1^2 + \chi_2^2). \tag{18}$$

The best fitting values of the parameters can be obtained by maximizing the likelihood function $L_{\rm tot}$.

4. Results and Conclusions

I sample the likelihood function $L_{\rm tot}$ by performing a Markov Chain Monte Carlo (MCMC) analysis using Python module *emcee* (Foreman-Mackey et al. 2013) and compute the one-dimensional (1D) marginalized best fitting values and 68% uncertainties of the parameters. The results are listed in Table 1. The two-dimensional (2D) contours and the 1D posterior probability distributions for the parameters, generated using the Python module GETDIST (Lewis 2019), are shown in Figures 2–5.

1. In the spatially flat Universe ($\Omega_k = 0$), with linear parameterization, i.e. $\eta(z) = 1 + \eta_0\, z$, the 1D marginalized best fit value of η_0 is $-0.0051^{+0.0677}_{-0.0621}$ which is in excellent agreement with the CDDR at a very high level of confidence. With nonlinear parameterization for $\eta(z)$, the 1D marginalized best fit value of η_0 is $-0.0921^{+0.0778}_{-0.0663}$. The value of η_0 shows no significant deviation from CDDR.
2. With a non-flat geometry, the 1D marginalized best fit value of η_0 for linear and nonlinear parametrizations is: $0.033^{+0.0749}_{-0.0702}$ and $-0.1205^{+0.0809}_{-0.0740}$ respectively. Again the value of η_0 with linear parameterization is in agreement with the CDDR within the 1σ confidence interval. With nonlinear parameterization too CDDR is true within the 2σ confidence interval. The data set provides a weak constraint on Ω_K but CDDR holds for a non-flat Universe with tight constraints on η_0 which is mildly dependent on Ω_K.

For a comparison, the results of some of the works with a model-independent approach are presented in Table 2.

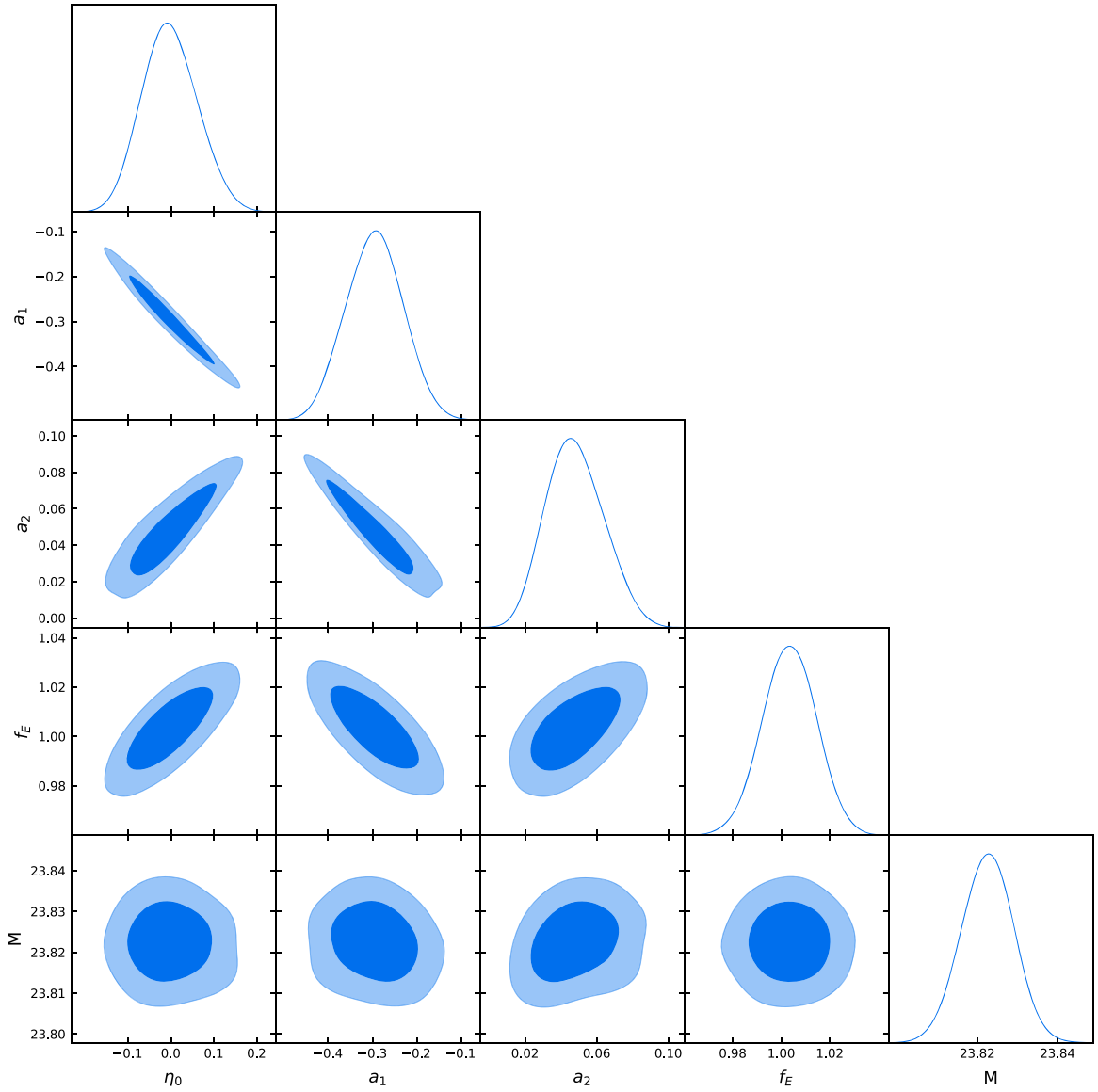

Figure 2. 1D posterior probability distributions and 2D confidence regions of the parameters in flat spacetime with $\eta(z) = 1 + \eta_0\, z$.

Table 1
1D Marginalized Best Fit Parameter Values and Uncertainties

With $\eta(z) = 1 + \eta_0\, z$					
Ω_K	η_0	a_1	a_2	$f_{\rm E}$	M
0	$-0.0051^{+0.0677}_{-0.0621}$	$-0.2942^{+0.0641}_{-0.0664}$	$0.0471^{+0.0176}_{-0.0154}$	$1.0033^{+0.0109}_{-0.0109}$	$23.8226^{+0.0063}_{-0.0066}$
$0.0567^{+0.0313}_{0.0374}$	$-0.0330^{+0.0749}_{-0.0702}$	$-0.2681^{+0.0712}_{-0.0731}$	$0.0438^{+0.0174}_{-0.0149}$	$1.0001^{+0.0118}_{-0.0106}$	$23.8233^{+0.0059}_{-0.0068}$
With $\eta(z) = 1 + \eta_0(z/1 + z)$:					
Ω_K	η_0	a_1	a_2	$f_{\rm E}$	M
0	$-0.0921^{+0.0778}_{-0.0663}$	$-0.2428^{+0.0421}_{-0.0486}$	$0.0301^{+0.0162}_{-0.0132}$	$0.9984^{+0.0083}_{-0.0082}$	$23.8286^{+0.0088}_{-0.0081}$
$0.1485^{+0.0948}_{-0.0952}$	$-0.1205^{+0.0809}_{-0.0740}$	$-0.2292^{+0.0519}_{-0.0500}$	$0.0278^{+0.0167}_{-0.0162}$	$1.0017^{+0.0086}_{-0.0092}$	$23.8309^{+0.0086}_{-0.0089}$

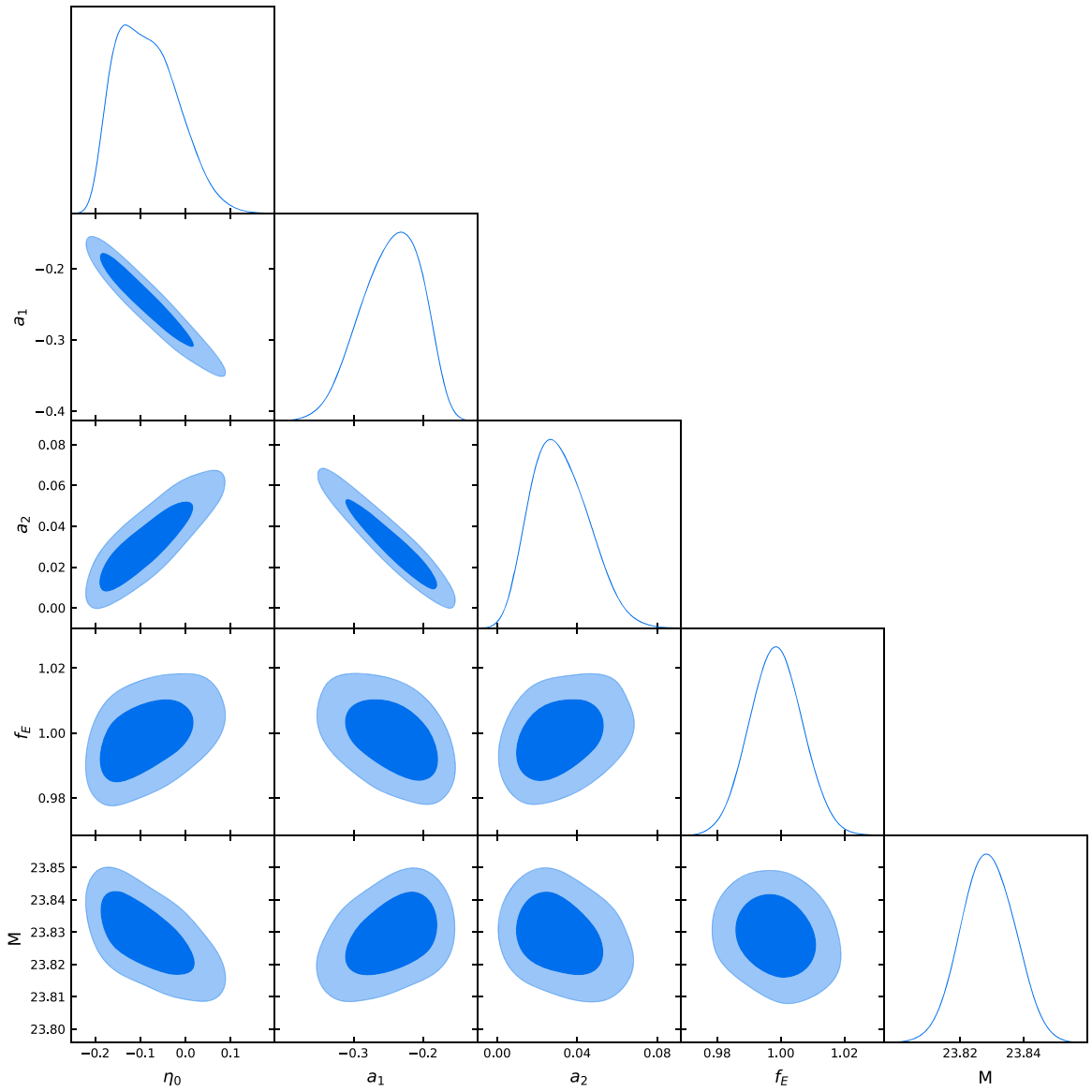

Figure 3. 1D posterior probability distributions and 2D confidence regions of the parameters in flat spacetime with $\eta(z) = 1 + \eta_0(z/1 + z)$.

Ruan et al. (2018) tested CDDR based on SGL and a reconstruction of the H II galaxy Hubble diagram using Gaussian processes. Xu et al. (2022) used the combination of BAO measurements and SNe Ia sample. They applied both an artificial neural network (ANN) method and binning the SNe Ia sample method to derive the values of luminosity distance at the redshifts of BAO measurements. Whereas, Wang et al. (2024) derived luminosity distance values at the redshifts of BAO measurements by binning and using Gaussian processes. Lyu et al. (2020) and Liao et al. (2016) tested CDDR by combining the SGL observations with SNe Ia data using linear parameterization for $\eta(z)$. They combine each SGL system with two SNe Ia events closest to the redshift of the source and lens with a difference not exceeding 0.005. Using the SIS lens mass model, Lyu et al. (2020) reported $\eta_0 = -0.161^{+0.062}_{-0.058}$, showing a moderate tension with the CDDR. In contrast, by choosing only those SGL systems which are found to be in better accordance with the SIS lens model and using the larger and updated SNe Ia data (Pantheon+), η_0 is consistent with 0 with high precision. The issue of finding the supernovae from the Pantheon+ data set whose redshift matches that of lens and source in each SGL system is overcome by reconstructing a continuous co-moving distance function $d(z)$, that best approximates the discrete observed data, using a polynomial fit. The best fit value of η_0 in a spatially flat Universe is consistent with the values reported in other works and with

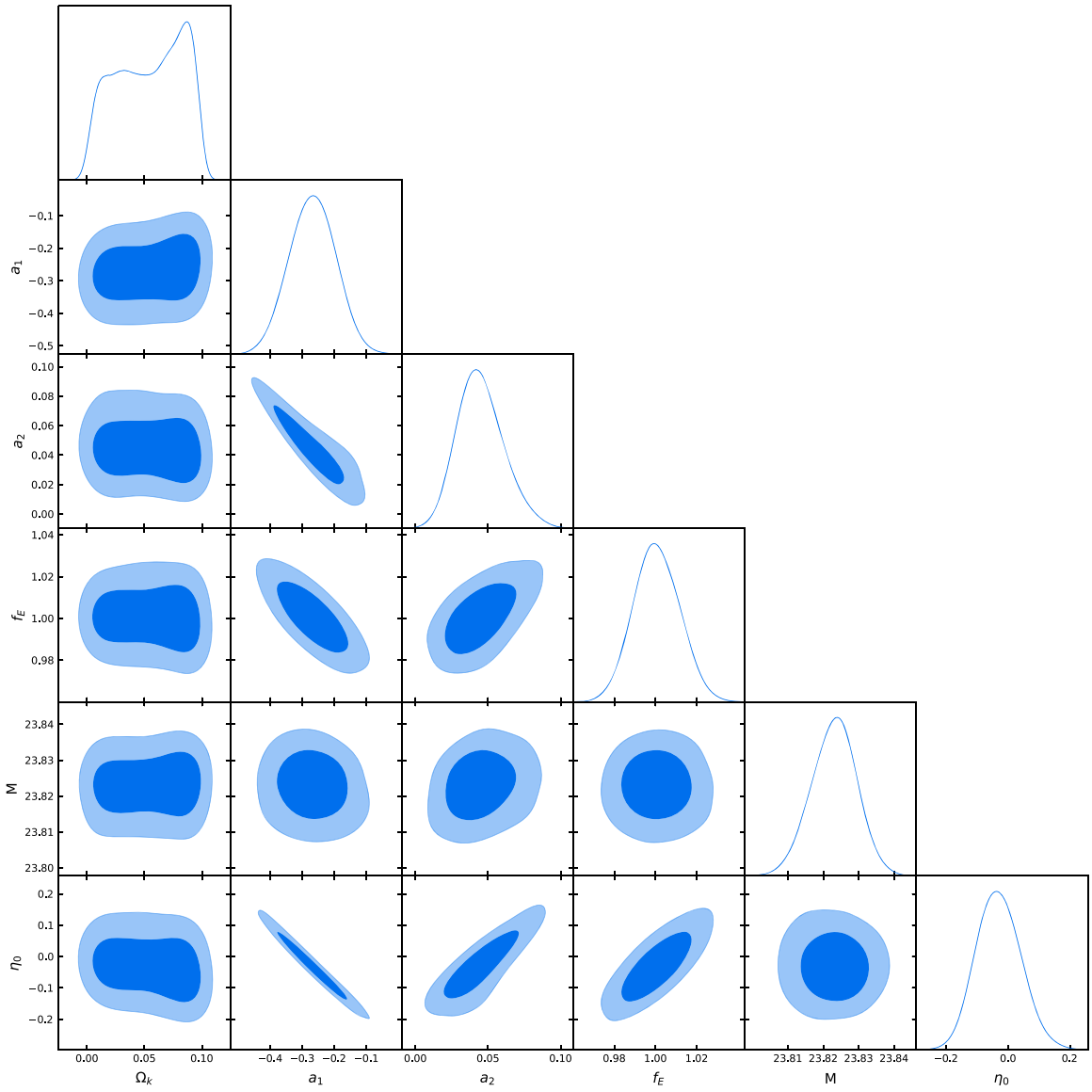

Figure 4. 1D posterior probability distributions and 2D confidence regions of the parameters in non- flat spacetime with $\eta(z) = 1 + \eta_0\, z$.

similar or better precision (Table 2). In addition, the method also confirms the validity of CDDR with a small confidence interval in the curved spacetime.

5. Discussion

CDDR is one of the fundamental relations in cosmology which plays a crucial role in astronomical observations. Any deviation from CDDR indicates that either the spacetime is not described by a metric theory of gravity or there is new physics beyond what we understand. With the availability of new improved observational data with better precision, it is important to test this relation. In this paper, using the latest SGL and SNe Ia Pantheon+ data jointly, I probe the validity of CDDR without considering any cosmological model. In most of the studies of CDDR so far, spatial flatness of spacetime is assumed. Whereas, using the distance sum rule along null geodesics in the FLRW metric, I test CDDR in a non-flat spacetime as well as a flat spacetime. The analysis shows that CDDR is valid at a very high level of confidence in the flat spacetime. In a non-flat spacetime too, CDDR is true within the 1σ confidence interval with a mild dependence of η_0 on Ω_K. To check the effect of parameterization, a nonlinear parameterization for $\eta(z)$ is used and found no significant deviation from CDDR. The high level of confidence achieved in the results is attributed to the improved SNe Ia observations with the covariance matrix incorporating all kinds of statistical and

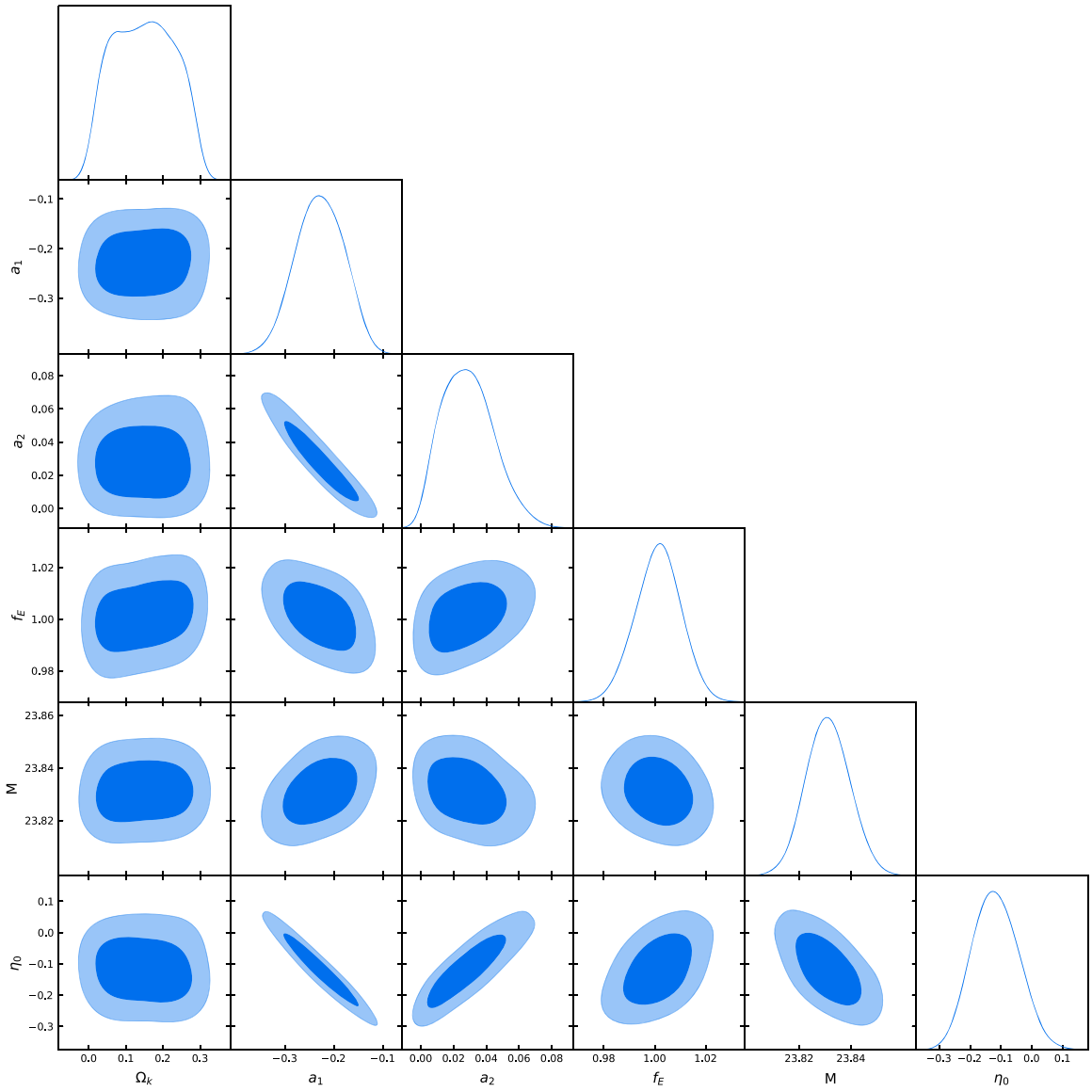

Figure 5. 1D posterior probability distributions and 2D confidence regions of the parameters in non-flat spacetime with $\eta(z) = 1 + \eta_0(z/1 + z)$.

Table 2
Best Fit Values of η_0 From Other Independent Studies

Data	$\eta_0(L)$	$\eta_0\ (N-L)$	References
SNe Ia + SGL	$-0.005^{+0.351}_{-0.251}$	⋯	Liao et al. (2016)
H II + SGL	$0.0147^{+0.056}_{-0.066}$	⋯	Ruan et al. (2018)
SNe Ia + SGL	$-0.161^{+0.062}_{-0.058}$	⋯	Lyu et al. (2020)
BAO + SNe Ia	$-0.064^{+0.057}_{-0.052}$	$-0.181^{+0.160}_{-0.141}$	Xu et al. (2022)
BAO + SNe Ia	$0.041^{+0.123}_{-0.109}$	$0.082^{+0.246}_{-0.214}$	Wang et al. (2024)
SNe Ia + SGL	$-0.0051^{+0.0677}_{-0.0621}$	$-0.0921^{+0.0778}_{-0.0663}$	This work

systematic uncertainties. Further, new powerful space and ground-based telescopes for imaging and spectroscopic observations helped to achieve better precision for SGL observations. The only limitation while using SGL data is the uncertainty about the mass distribution in the lens. To mitigate the impact of an imprecisely known mass distribution, I selected only those lensing systems which are proved to be in accordance with the SIS lens model. Also, the model-independent method used in the work helped to avoid the unknown systematics associated with the models.

The results for both flat and non-flat spacetime establish the CDDR all the way out to $z \sim 2.3$. However, it is important to test CDDR at higher redshifts up to the last scattering surface. Recently a large number of high-redshift quasars have been detected with redshifts between 4.44 and 6.53, using the Dark Energy Spectroscopic Instrument (DESI; Yang et al. 2023). The multiple measurements of high-redshift quasars can be used to estimate luminosity distances from the relation between the ultraviolet (UV) and X-ray luminosities of quasars.

Whereas, angular diameter distances can be obtained from the compact structures in intermediate luminosity radio quasars. Thus, two different cosmological distances from the same kind of object at high redshifts can be determined and compared (Zheng et al. 2020). Further, recent detection of gravitational wave (GW) signals by LIGO and Virgo detectors has heralded the start of GW astronomy and the multi-messenger astronomy era (Abbot et al. 2016a, 2016b, 2017). These "standard sirens" could provide the absolute luminosity distance of the event without any calibration, as GWs propagate freely through a perfect fluid without any absorption or dissipation (Schutz 1986). Combining the GW data with SGL or BAO data (for angular diameter distances) can give a more precise test of CDDR. Theoretically, third generation GW detectors, such as the Einstein Telescope (ET), could detect GW signals up to redshift $z \sim 2$ for neutron star—neutron star mergers and $z \sim 5$ for black hole—neutron star merger systems (Cai & Yang 2017). Also, a possible detection of strong GW lensing can provide simultaneous measurements of both the luminosity and angular diameter distances which in turn can be used to probe CDDR (Arjona et al. 2021). However, we should wait for the data from ET until the statistics and redshift coverage will be sufficient to get competitive results.

Acknowledgments

I thank Kshitiz Singh for helping me with the codes and the anonymous referee for constructive comments that helped to improve the manuscript.

Data Availability

The data sets used in this work are available in the public domain. For SGL data, check https://doi.org/10.1093/mnras/stz1902. Pantheon+ SNe Ia sample is available at: https://github.com/PantheonPlusSH0ES/PantheonPlusSH0ES.github.io.

Funding and/or Conflicts of Interests/Competing Interests

This work is done independently and no funds, grants, or other support was received. There are no conflicts of interests that are relevant to the content of this article.

References

Abbot, B. P., Abbot, R., Abbot, T.D., et al. 2016a, PhRvL, 116, 061102
Abbot, B. P., Abbot, R., Abbot, T.D., et al. 2016b, PhRvL, 116, 241103
Abbot, B. P., Abbot, R., Abbot, T.D., et al. 2017, PhRvL, 118, 221101
Arjona, R., Lin, H.-N., Nesseris, S., & Tang, L. 2021, PhRvD, 103, 103513
Bassett, B. A., & Kunz, M. 2004, PhRvD, 69, 101305
Brout, D., Scolnic, D., Popovic, B., et al. 2022, ApJ, 938, 110
Cai, R. G., & Yang, T. 2017, PhRvD, 95, 044024
Cao, S., Pan, Y., Biesiada, M., Godlowski, W., & Zhu, Z.-H. 2012, JCAP, 3, 16
Cao, S., Biesiada, M., Gavazzi, R., Piórkowska, A., & Zhu, Z.-H. 2015, ApJ, 806, 185
Cao, S., Biesiada, M., Yao, M., & Zhu, Z.-H. 2016, MNRAS, 461, 2192
Cao, S., & Zhu, Z. H. 2011, SCPMA, 54, 2260
Cao, S., Biesiada, M., Zheng, X., & Zhu, Z.-H. 2016, MNRAS, 457, 281
Cappellari, M., Bacon, R., Bureau, M., et al. 2006, MNRAS, 366, 1126
Chen, Y., Li, R., & Shu, Y. 2019, MNRAS, 488, 3745
Collet, T., Montanari, F., & Räsänen, S. 2019, PhRvL, 123, 231101
Corasaniti, P. S. 2006, MNRAS, 372, 191
Ellis, G. F. R., Poltis, R., Uzan, J.-P., & Weltman, A. 2013, PhRvD, 87, 103530
Etherington, I. 1933, The London Edinburgh, and Dublin Philosophical Magazine and Journal of Science, 15, 761
Foreman-Mackey, D., Hogg, D. W., Lang, D., & Goodman, J. 2013, PASP, 125, 306
Gahlaut, S. 2024, Prama, 98, 22
Holanda, R. F. L., & Busti, V. C. 2014, PhRvD, 89, 103517
Holanda, R. F. L., Lima, J. A. S., & Ribeiro, M. B. 2011, A&A, 528, L14
Holanda, R. F. L., Lima, J. A. S., & Ribeiro, M. B. 2012, A&A, 538, A131
Holanda, R. F. L., Carvalho, J. C., & Alcaniz, J. S. 2013, JCAP, 04, 027
Jorgensen, I., Franx, M., & Kjaergaard, P. 1995a, MNRAS, 273, 1097
Jorgensen, I., Franx, M., & Kjaergaard, P. 1995b, MNRAS, 276, 1341
Kessler, R., & Scolnic, D. 2017, ApJ, 836, 56
Kochanek, C. S. 1992, ApJ, 397, 381
Kochanek, C. S., Falco, E. E., Impey, C. D., et al. 2000, ApJ, 543, 131
Koopmans, L. V. E., Treu, T., Bolton, A. S., Burles, S., & Moustakas, L. A. 2006, ApJ, 649, 599
Koopmans, L. V. E., Bolton, A., Treu, T., et al. 2009, ApJL, 703, L51
Lewis, A. 2019, arXiv: 1910.13970
Li, Z., Wu, P., & Yu, H. 2011, ApJL, 729, L14
Li, Z., Wu, P., Yu, H., & Zhu, Z.-H. 2013, PhRvD, 87, 103013
Liao, K., Li, Z., Cao, S., et al. 2016, ApJ, 822, 74
Lyu, M. Z., Li, Z. X., & Xia, J.-Q. 2020, ApJ, 888, 32
Melia, F. 2018, MNRAS, 481, 4855
Melia, F., Wei, J.-J., & Wu, X.-F. 2015, AJ, 149, 2
Nesseris, S., & Bellido, J. G. 2012, JCAP, 11, 033
Ofek, E. O., Rix, H. W., & Maoz, D. 2003, MNRAS, 343, 639
Peebles, P. J. E. 1993, Principals of Physical Cosmology (Princeton, NJ: Princeton Univ. Press)
Qi, J. Z., Zhao, J. W., Cao, S., Biesiada, M., & Liu, Y. 2021, MNRAS, 503, 2179
Rana, A., Jain, D., Mahajan, S., & Mukherjee, A. 2016, JCAP, 07, 026
Rana, A., Jain, D., Mahajan, S., Mukherjee, A., & Holanda, R. F. L. 2017, JCAP, 07, 010
Räsänen, S., Bolejko, K., & Finoguenov, A. 2015, PhRvL, 115, 101301
Ratnatunga, K. U., Griffiths, R. E., & Ostrander, E. J. 1999, AJ, 117, 2010
Riess, A. G., Yuan, W., Macri, L. M., et al. 2022, ApJL, 934, L7
Ruan, C.-Z., Melia, F., & Zhang, T.-J. 2018, ApJ, 866, 31
Schneider, P., Kochanek, C., & Wambsganss, J. 2006, Gravitational Lensing: Strong, Weak and Micro (Berlin Heidelberg: Springer-Verlag)
Schutz, B. F. 1986, Natur, 323, 310
Scolnic, D., Brout, D., Carr, A., et al. 2022, ApJ, 938, 113
Shafieloo, A., Majumdar, S., Sahni, V., & Starobinsky, A. A. 2013, JCAP, 04, 042
Treu, T., Koopmans, L. V. E., Bolton, A. S., Burles, S., & Moustakas, L. A. 2006, ApJ, 650, 1219
Wang, M., Fu, X., Xu, B., et al. 2024, EPJC, 84, 702
Wei, J. J., & Melia, F. 2020, ApJ, 897, 127
Xu, B., Wang, Z., Zhang, K., et al. 2022, ApJ, 939, 115
Yang, J., Fan, X., Gupta, A., et al. 2023, ApJS, 269, 27
Zheng, X., Liao, K., Biesiada, M., et al. 2020, ApJ, 892, 103